Aerodynamic Drag Reduction and Flow Control of a Simplified Road Vehicle

W. Zeidan[a], N. Mazellier[a], E. Guilmineau[b], A. Kourta[a]

a. Univ. Orleans, INSA CVL, PRISME, EA 4229, F 45072, Orleans, France
(PRISME) Universite d'Orleans : EA4229, INSA Centre Val de Loire-France
b. LHEEA, CNRS 6598, Ecole Centrale de Nantes (ECN - CNRS) CNRS : UMR6598
ECOLE CENTRALE DE NANTES 1 rue de la Noe BP 92101 44321 Nantes Cedex 03, France
wassim.zeidan@univ-orleans.fr nicolas.mazellier@univ-orleans.fr
emmanuel.guilmineau@ec-nantes.fr azeddine.kourta@univ-orleans.fr

Résumé :

La distribution de pression à la base d'un modèle à dos carré (corps d'Ahmed) est mesurée expérimentalement pour évaluer les effets des volets horizontaux mobiles, dans diverses conditions de fonctionnement, en changeant la turbulence de flux libre et l'angle de lacet. Le coefficient de traînée aérodynamique déduit par un bilan des forces et la distribution de pression ont été calculés et présentés pour différents cas au nombre de Reynolds $Re_H = 7.6 \times 10^5$ selon la vitesse du courant libre et la hauteur du modèle. Les effets directs des volets sur les coefficients de traînée et la réduction de la traînée ont été obtenus, et de grands effets de la grille ont été observés et discutés.

Abstract :

The pressure distribution field at the base of a square-back model (Ahmed body) is measured experimentally to assess the effects of movable horizontal flaps, in various operating conditions by changing the free-stream turbulence and the yaw angle. Aerodynamic drag coefficient inferred by a force balance and the pressure distribution have been calculated and presented for different cases at Reynolds number $Re_H = 7.6 \times 10^5$ depending on the free stream velocity and the height of the model. Direct effects of the flaps on the drag coefficients and a drag reduction were achieved, as well as great effects of the grid were observed and discussed.

Keywords: Aerodynamics, Drag reduction, Flow control

1 Introduction

Upgrades in fuel economy in transportation require the development of breakthrough technologies to achieve drag reduction. Indeed, a huge portion of the power consumption is caused by aerodynamic forces that oppose to the motion of vehicles such as trucks and cars on the highway. Zulfa et al. [4] showed the linear relation between aerodynamic drag reduction and fuel saving for heavy vehicles. Wide range of flow control strategies based on the use of flaps, spoilers or deflectors is available in literature,

most of them using fixed devices. Browand et al. [2] showed a field of tests on large heavy square-back vehicles that shows the effects of flaps on the fuel saving. Moreover, Capone et al. [3] benefit from the combination between horizontal and vertical flaps to achieve a drag reduction around 5%. Khaligi et al. [5] achieved a drag reduction by using splitters at the base of a square-back aerodynamic model, whilst Lucas et al. [6] used a base cavity which is comparable with the combination of horizontal and vertical flaps to study drag reduction. This raises the problem of an optimization process which is only relevant for a given set of operating conditions. These conditions are likely to change, the latter which makes a more attractive solution by using adaptive flaps, Mazellier et al, 2012 [7]. Our study will focus on the drag reduction by using movable horizontal flaps installed at the base of Ahmed body model.

2 Experimental Setup

Ahmed Body: The experimental program exploit the full-scale Ahmed body used in Ahmed et al. [1], length, height and width being respectively L=1044mm, H=288mm, W=389mm Fig. 2, within a tunnel blockage of 2.8%. For all tests, the ground clearance was set at 45mm (15% of the model height). The model was mounted via a plate located 0.47m from ground within a rotation ability in order to be aligned with the yaw angle. The x-axis is aligned with the stream-wise direction, z-axis is vertical and positive upwards, and the y-axis followed the right handed coordinate system, the origin is at the bottom of the base of the model at the mid wheelbase. Fig. 1

The wind tunnel: All the experiments were carried out in the "Lucien Malavard" closed-loop wind tunnel of the PRISME laboratory at the University of Orleans, France. The test section is 2m by 2m wide, and 5m long, with a free-stream turbulence intensity less than 0.4%. The free-stream velocity was chosen, $U_\infty = 40$m/s, which corresponds to Reynolds number based on the height of the model and free-stream velocity $Re_H = 7.6\times10^5$. The boundary layer thickness was measured to be $\delta_{99} = 28.8$mm.

Balance measurements: The aerodynamic forces were measured by an external strain gauge balance, located under the working section of the tunnel. The chosen sampling frequency is $f_s = 1000$Hz for $time = 30$min. The measured values of the forces have been normalized using the following equation:

$$C_x = \frac{Force}{0.5\,\rho\,S\,U_\infty^2} \tag{1}$$

where ρ is the air density and S is the projected model frontal area (S=0.112m^2)

Pressure measurements: The pressure at the model base was measured by settling the back-square face with a grid of 81 pressure taps connected by a venyl tube (length 600mm with internal diameter $d = 1.56$mm) and with a manufacturer quoted accuracy of ±6Pa.

Moreover, the taps were located with a finer distribution close to the body edges, to get more accuracy in the pressure representation. In addition, two MicroDAQ pressure scanners were used with a sampling frequency $F_s = 50$Hz for $time = 30$min. The pressure coefficients were calculated according to the following equation:

$$C_{pb} = \frac{p - p_\infty}{0.5\,\rho\,S_b U_\infty^2} \tag{2}$$

where p_∞ is the free-stream static pressure, S_b is the area covered by the pressure taps. Accordingly, the base drag was estimated by integrating the measured pressure field eq. 3:

$$\bar{C}_{db} = -\frac{1}{S_b} \iint_S \bar{C}_{pb}\, dS \tag{3}$$

where $\bar{C}_{pb}$ is the time averaged estimated pressure coefficient.

Flap installation: Horizontal flaps were installed at the rear of the body to study the effects on the drag coefficients to have a view about drag reduction. In this study, the normalized length of the flaps is l/L = 10%. Two configurations are studied using one or a combination of two flaps, respectively.

Grid installation: Fig. 1 shows the grid installation. The grid is 2m by 2m installed 1.5m upstream of the leading edge of the raised floor. Cell size is 30 × 30cm (distance between centers of the bars) with 2.5cm for bar thickness. The installation of the grid came to rain force into more realistic conditions. The turbulent intensity achieved by this grid is I=6 %.

These configurations gives a better understanding about the drag reduction mechanism Fig. 1: one free movable flap placed at the top of the base of the model, while second configuration placed at the top and bottom of the base.

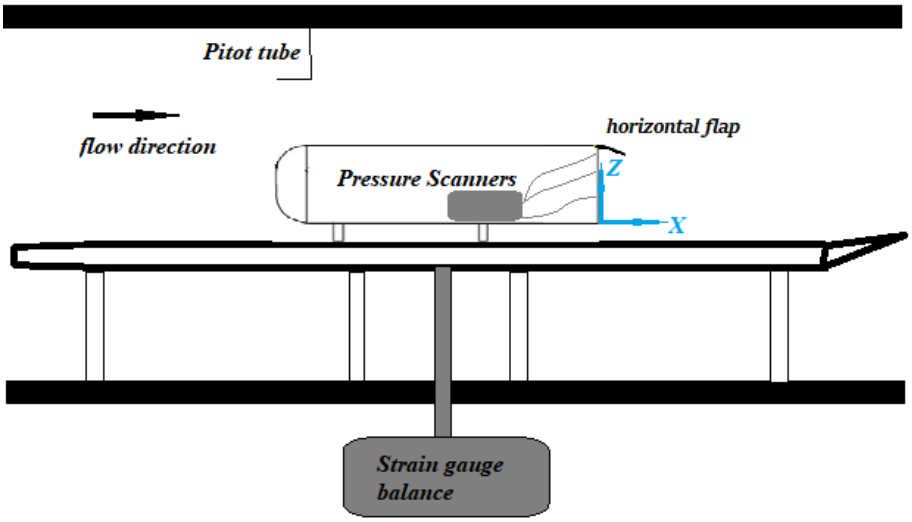

(a)

(b) (c)

Figure 1: **(a)** Experimental setup, **(b)** Configuration (1) one horizontal movable flap at the top, **(c)** Configuration (2) two horizontal movable flaps at the top and the bottom.

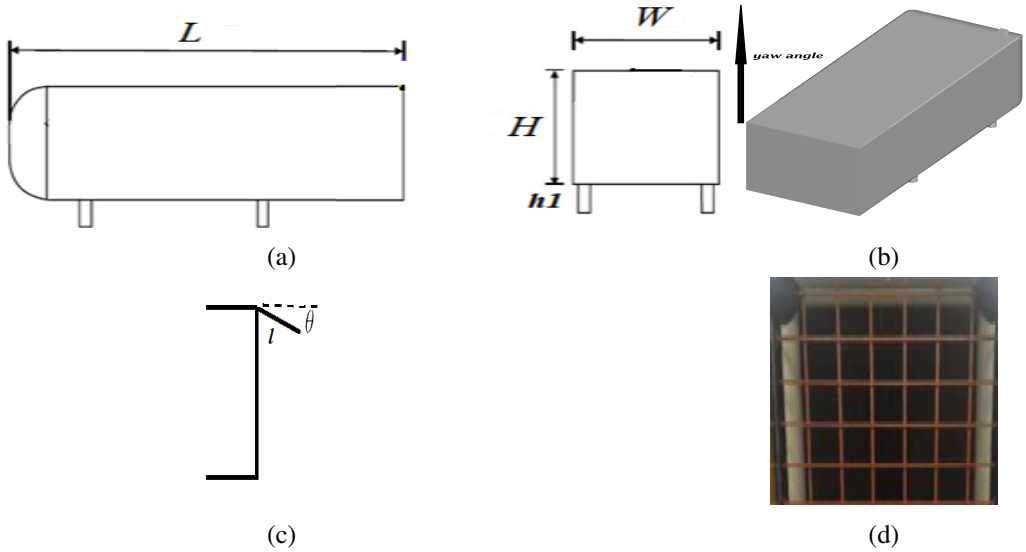

(a) (b)

(c) (d)

Figure 2: (a) Ahmed Body model length $L = 1044mm$, height $H = 288mm$, width $W = 389mm$ and ground clearance $h_1 = 45mm$, (b) Yaw angle, (c) Flap position, (d) Grid .

3 Results and Discussions

The time-averaged drag reduction are shown in table 1, where the drag reduction was calculated according to eq. 4.

$$DR\ (\%) = 1 - \frac{Cd_{with\ Flaps}}{Cd_{Reference}} \tag{4}$$

where $Cd_{with\ Flaps}$ is the drag coefficient with the installed flaps and $Cd_{Reference}$ is the drag coefficient with the installed flaps. At zero yaw angle, table 1 shows the drag reduction for Ahmed body using movable flaps with and without presence of grid. The drag reduction by using the grid itself for the reference case (without flaps) is $4\,\%$, while $9\,\%$ for total DR achieved by using the two free movable flaps in the presence of grid.

	one free flap	two free flaps	one free(with grid)	two free(with grid)
DR_{base}	8%	8%	7%	13%
DR_{total}	6%	6%	5%	9%

Table 1: Drag Reduction for one and two horizontal free movable flaps, with and without grid at yaw=0

Table 2 shows the drag reduction for the two movable flaps with and without grid at yaw angle $4°$. It is clearly notable that the effect of flaps decreased with grid as the yaw angle increased.

	two free flaps	two free(with grid)
DR_{base}	$13\,\%$	$13\,\%$
DR_{total}	$8\,\%$	$3\,\%$

Table 2: Drag Reduction for one and two horizontal free movable flaps, with and without grid at yaw=$4°$

Fig. 3 shows the pressure coefficient distribution at the base of the model, Fig. 3a is for two free movable flap installation at yaw angle$0°$ while Fig. 3b presents same installation but at yaw angle $4°$.

Huge difference in terms of pressure distribution due to the fact of yaw angle $4°$. This fact could be seen more clearly on Fig. 4a (high symmetric distribution for pressure at zero yaw angle).

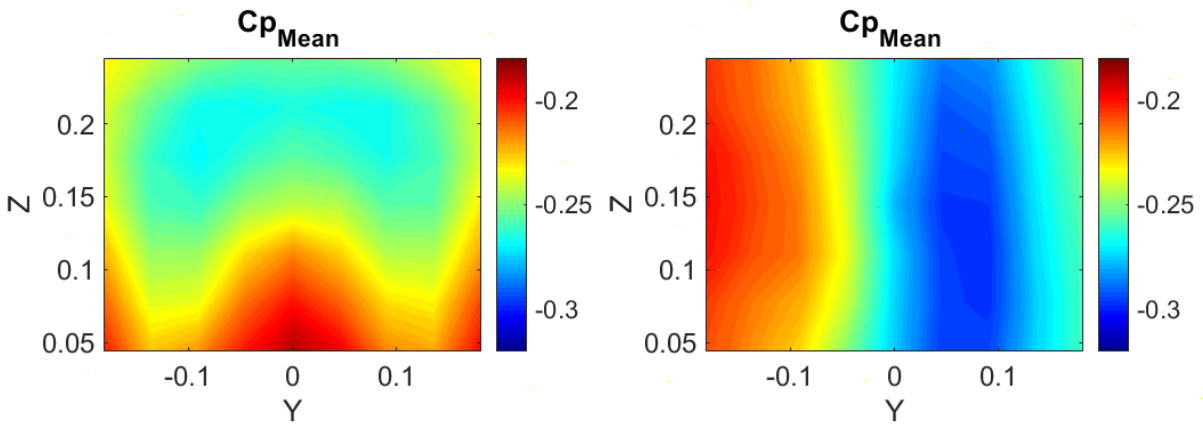

(a) (b)

Figure 3: Pressure distribution at the base by using 2 free flaps at zero yaw **(a)** , yaw angle 4° **(b)**

Consistency between base and total drag reduction is studied and shown in Fig. 4b, where this consistency confirms the importance given to base drag reduction and its high effect on total drag, as it represents 80% from the total drag of the model as measured in the experiment.

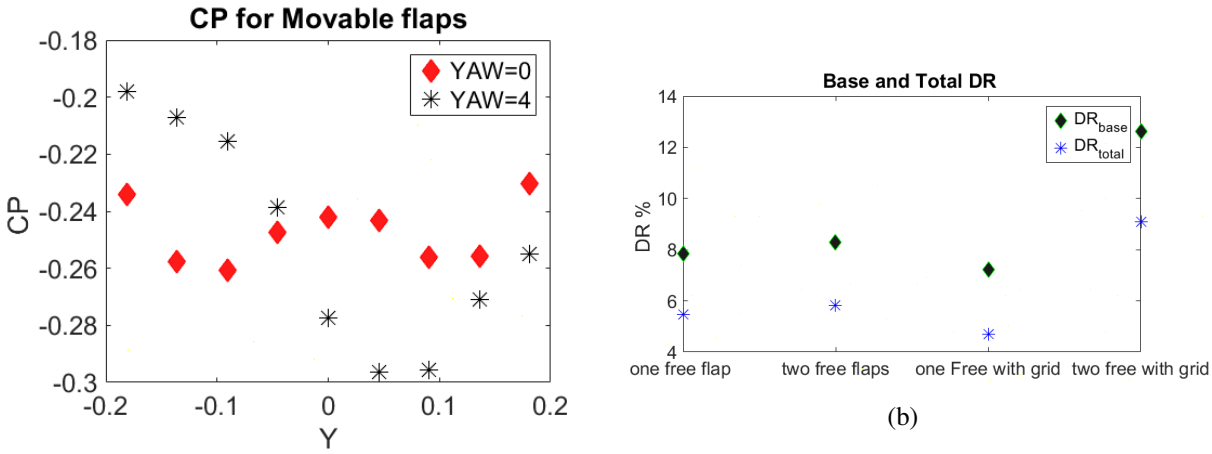

(a) (b)

Figure 4: **(a)** Pressure coefficient at the base for $0°$ and $4°$ yaw angle,**(b)** Total and base drag reduction for different installation (one free movable flap, two free movable flaps, one free with grid and two free with grid).

4 Conclusion

The prior experimental studies make use of the of balance and pressure measurements of the Ahmed body model with and without flaps at Reynolds number $Re_H = 7.6 \times 10^5$, focusing on the drag coefficient behavior to study the drag reduction . Our study extends the work of Mazellier et al.[7] by considering movable flaps playing on external conditions as grid installation and yaw angle, where combining the use of flap and grid achieved highest drag reduction at zero yaw angle. Nevertheless, pressure distribution were addressed for zero and yaw angle $4°$.

References

[1] S.R. Ahmed, G. Ramm, and G. Faltin. Some salient features of the time-averaged ground vehicle wake. In *SAE Technical Paper*. SAE International, 02 1984.

[2] F. Browand, C. Radovich, and M. Boivin. Fuel savings by means of flaps attached to the base of a trailer: Field test results. In *SAE Technical Paper*. SAE International, 04 2005.

[3] A. Capone and G. Romano. Investigation on the effect of horizontal and vertical deflectors on the near-wake of a square-back car model. *Journal of Wind Engineering and Industrial Aerodynamics*, 185:57 – 64, 2019.

[4] Z. Kassim and A. Filippone. Fuel savings on a heavy vehicle via aerodynamic drag reduction. *Transportation Research Part D: Transport and Environment*, 15(5):275 – 284, 2010.

[5] B. Khalighi, S. Zhang, C. Koromilas, S. R. Balkanyi, Luis P. Bernal, G. Iaccarino, and P. Moin. Experimental and computational study of unsteady wake flow behind a bluff body with a drag reduction device. *SAE Transactions*, 110:1209–1222, 2001.

[6] J. Lucas, O. Cadot, V. Herbert, S. Parpais, and J. Delery. A numerical investigation of the asymmetric wake mode of a squareback ahmed body effect of a base cavity. *Journal of Fluid Mechanics*, 831:675 – 679, 2017.

[7] N. Mazellier, A. Feuvrier, and A. Kourta. Biomimetic bluff body drag reduction by self-adaptive porous flaps. *Comptes Rendus Mecanique*, 340(1):81 – 94, 2012. Biomimetic flow control.